

1 **Annual variability and regulation of methane and sulfate fluxes in**
2 **Baltic Sea estuarine sediments**

3
4
5
6
7
8
9
10
11
12
13
14
15
16
17
18
19
20
21
22
23
24
25
26
27
28
29

Joanna E. Sawicka and Volker Brüchert

Department of Geological Sciences, Stockholm University, Stockholm, 10691, Sweden

Correspondence to: Volker Brüchert (volker.bruchert@geo.su.se)

30 **Abstract.** Marine methane emissions originate largely from near-shore coastal systems, but emission
31 estimates are often not based on temporally well-resolved data or sufficient understanding of the
32 variability of methane consumption and production processes in the underlying sediment. The
33 objectives of our investigation were to explore the effects of seasonal temperature, changes in benthic
34 oxygen concentration, and historical eutrophication on sediment methane concentrations and benthic
35 fluxes at two type localities for open-water coastal versus eutrophic, estuarine sediment in the Baltic
36 Sea. Benthic fluxes of methane and oxygen, sediment porewater concentrations of dissolved sulfate,
37 methane, and ³⁵S-sulfate reduction rates were obtained over a 12-month period from April 2012 to
38 April 2013. Benthic methane fluxes varied by factors of 5 and 12 at the offshore coastal site and the
39 eutrophic estuarine station, respectively, ranging from 0.1 mmol m⁻²d⁻¹ in winter at an open coastal site
40 to 2.6 mmol m⁻²d⁻¹ in late summer in the inner eutrophic estuary. Total oxygen uptake (TOU) and ³⁵S-
41 sulfate reduction rates (SRR) correlated with methane fluxes showing low rates in the winter and high
42 rates in the summer. The highest porewater methane concentrations also varied by factors of 6 and 10
43 over the sampling period with lowest values in the winter and highest values in late summer-early
44 autumn. The highest porewater methane concentrations were 5.7 mM a few centimeters below the
45 sediment surface, but never exceeded the in-situ saturation concentration. 21 – 24% of the total sulfate
46 reduction was coupled to anaerobic methane oxidation lowering methane concentrations below the
47 sediment surface far below the saturation concentration. The data imply that bubble emission likely
48 plays no or only a minor role for methane emissions in these sediments. The changes in porewater
49 methane concentrations over the observation period were too large to be explained by temporal changes
50 in methane formation and methane oxidation rates due to temperature alone. Additional factors such as
51 regional and local hydrostatic pressure changes and coastal submarine groundwater flow may also
52 affect the vertical and lateral transport of methane.

53

54 **Keywords** Methane cycling, coastal and estuarine sediment, seasonality

55 **1 Introduction**

56 The world's estuaries have been suggested to emit between 1.8 and 6.6 Tg CH₄ y⁻¹ to the atmosphere
57 (Borges and Abril, 2011; Amouroux et al 2002, Marty et al., 2001; Middelburg et al., 2002; Sansone et
58 al., 1999; Upstill-Goddard et al., 2000), a considerable portion of the estimated total oceanic emissions
59 of 10-30 Tg CH₄ y⁻¹ (Judd, 2004; Etiope et al., 2008; Kirschke et al., 2013). As other globally upscaled
60 estimates of emissions, these estimates also have considerable uncertainties. In the case of estuaries, a
61 major cause of the uncertainty are relatively few spatially and temporally resolved measurements of
62 anaerobic carbon degradation measurements in sediments and measurements of methane fluxes from
63 sediments. In estuarine waters methane can be derived from underlying anoxic sediments, transported
64 laterally due to freshwater or sewage discharge, seepage of methane-rich groundwater, or it can be
65 derived from near-shore aquatic plants (Borges and Abril, 2011). The amount of sedimentary methane
66 production in estuaries is a function of organic matter availability, bottom water oxygen concentrations,
67 and the salinity of the estuary. Methane production is generally greater in low-salinity estuaries because
68 of lower sulfate availability to promote bacterial sulfate reduction (Borges and Abril, 2011). Methane
69 fluxes from estuarine sediments are characterized by significant spatial and temporal variability
70 (Borges and Abril 2011). Temporal patterns show that concentrations and fluxes of CH₄ are generally
71 higher in the warmer season and low in the colder season (Crill et al., 1983, Martens and Klump, 1984,
72 Musenze et al., 2014; Reindl and Bolalek, 2014). Notably, very few studies have considered CH₄ fluxes
73 in high-latitude environments during snow- and ice-covered periods. While shallow systems within the
74 tidal range derive a significant amount of the methane flux from ebullition (Martens and Klump, 1984),
75 groundwater discharge, tidal pumping, and transport by aquatic plants (Middelburg et al., 2002;
76 Kristensen et al 2008), the transport from deeper systems such as fjords and fjärds is thought to occur
77 largely by molecular diffusion (Abril and Iversen, 2002, Sansone et al., 1998).

78 Globally more than 90% of methane produced in marine sediments is estimated to be oxidized by the
79 anaerobic oxidation of methane (AOM), mostly in the sulfate-methane transition zone (Knittel and

80 Boetius, 2009, Martens and Berner, 1974; Jørgensen and Parkes, 2010). It is not known how much
81 methane is oxidized by AOM in estuarine sediments. In addition, up to 90% of the remaining methane
82 that reaches the sediment surface may be oxidized aerobically at the sediment surface or in the water
83 column (Reeburgh, 2007). Yet, methane concentrations in estuarine waters are almost always higher
84 than the atmospheric equilibrium concentration indicating that microbial oxidation processes and
85 physical exchange with the atmosphere in estuaries are relatively inefficient in removing methane.
86 Despite its obvious importance, only few studies have specifically addressed anaerobic oxidation of
87 methane by sulfate and aerobic oxidation in estuarine environments (e.g., Treude et al., 2005, Thang et
88 al., 2013).

89 The objective of this study was therefore to further elucidate mechanisms behind temporal variability
90 of methane fluxes in a high-latitude coastal and estuarine environment with strong seasonal temperature
91 variability, winter ice cover, and variable degree of eutrophication stress. These data fill an important
92 gap of global inventories of nearshore sediment methane dynamics and help improve our mechanistic
93 understanding of methane emissions from marine near-shore systems. We determined porewater
94 concentrations of methane and sulfate, measured sulfate reduction rates with the ³⁵S-sulfate tracer
95 method, and conducted core incubations to determine benthic fluxes of methane and oxygen at two
96 deep stations of a low-salinity Baltic Sea estuary inside and at the opening of the estuary to the Baltic.
97 Investigations were carried out over four seasons to capture the annual variability of chemical and
98 biological conditions at the sediment surface and their influence on methane dynamics.

99

100 **2 Materials and methods**

101 **2.1 Site description**

102 Himmerfjärden (Figure 1) is a fjord-type estuary with a surface area of 174 km², a volume of
103 2968 x 10⁶ m³, and a N-S bottom water salinity gradient increasing from 5.5‰ in the inner part to
104 7.0‰ at the opening to the Baltic. It is morphologically characterized by four basins, divided by sills

105 and has a low flushing rate of about 0.025/day (Savage and Elmgren, 2010). The freshwater discharge
106 is small compared to the exchange with the open Baltic and was estimated to be 23 m³/s on average in
107 2012 comprising land run-off and precipitation (30% and 21%, respectively), outflow from Lake
108 Mälaren from the north (19%) and the river Trosaån (23%), and discharge from a sewage treatment
109 plant (6%) (Larsson et al., 2012). The sewage treatment plant, built in the early 1970s, treats sewage
110 water from ca. 314,000 inhabitants of the southern Stockholm metropolitan area, and its inorganic
111 effluent is discharged mainly in the form of inorganic nitrogen and phosphorus to the inner basins
112 (Savage and Elmgren, 2010). In 2012, the sewage treatment contributed 45% of the total phosphorus
113 and 57% of the total inorganic nitrogen discharge to the northern Himmerfjärden area (Larsson et al.,
114 2012) and discharged 1676 tons carbon (measured as chemical oxygen demand COD) (Stridh, 2012).
115 The estuary undergoes thermohaline stratification during late summer and autumn, especially in the
116 inner part, which experiences regular seasonal bottom water hypoxia. The tidal range is low (few cm)
117 and relatively cold bottom waters (1.5 - 9°C) dominate throughout the year. Water level can vary
118 annually by about 50 cm depending on local wind and hydrographic conditions. Late-summer-early fall
119 bottom water hypoxia has also been reported occasionally for the outer basins of the estuary, when
120 winds are weak and circulation is inhibited (Elmgren and Larsson, 1997). Sedimentation areas in
121 Himmerfjärden can be divided into accumulation and transport bottoms (Jonsson et al., 2003). About
122 21% of the sediment surface in Himmerfjärden is classified as accumulation bottoms of particulate
123 material and receives 3.3-9 mol C m⁻² y⁻¹ (Thang et al., 2013; Karlsson et al., 2010).

124 Bottom water and sediment samples were taken from a station in the inner part of
125 Himmerfjärden, Station H6, and from a station located outside the estuary, Station B1 (Figure 1).
126 Samples were collected in April, August, October 2012, and in February 2013. In addition, in April
127 2013 whole-core incubations were performed to determine methane and oxygen fluxes to record a full
128 year of seasonal variability. Station B1 has soft, olive grey, muddy sediment with a 1-2 cm-thick rusty
129 brown surface layer that was present year round, while the sediment at station H6 is soft, laminated
130 black mud with a 1-2 mm thin brown surface layer that occurred only during the winter and spring.

131 Sediment accumulation rates range from 0.98 cm yr⁻¹ in the innermost part of the estuary to 0.77 cm yr⁻¹
132 in the outer part of the estuary (Thang et al., 2013).

133

134 **2.2 Sample collection**

135 Sediments with well-preserved sediment surfaces were collected with a Multicorer in acrylic tubes (9.5
136 cm diameter) to 40 cm depth to determine ³⁵S-sulfate reduction rates, porosity, and the porewater
137 constituents methane and sulfate. Additional cores were collected for sediment core incubations.
138 Porewater methane samples were immediately collected on-board from the cores as described below.
139 The other cores were capped with rubber stoppers, transported to the marine laboratory on the island of
140 Askö within 90 minutes and kept cold at bottom water temperatures for later experiments and
141 subsampling. In February 2013, ice partially covered Station B1 and there was complete ice cover at
142 Station H6, and sampling was only possible after ice breaking. For whole-core incubations, 30 l of
143 bottom water was collected with a 5 liter HydroBios bottle and kept cold until for the experiments.
144 Temperature, salinity, and oxygen concentrations were determined with a handheld WTW Oxygen
145 meter directly in the water overlying the sediment cores.

146

147 **2.3 Organic carbon concentrations and porosity**

148 Concentrations of organic carbon were determined for the topmost cm of sediment on freeze-dried
149 sediment with a Fisons CHN elemental analyzer after treatment with 1M HCl to remove inorganic
150 carbon. Water content (%) was determined by drying 5 ml of sediment at 105°C and calculating the
151 percent loss after drying.

152

153 **2.4 Methane analysis**

154 Samples for methane were collected directly through the side of taped, pre-drilled core liners and taken
155 in 2-cm intervals minutes after the core was retrieved on deck. The core sampling method used in this

156 study permits complete sampling and preservation of porewater methane within 5 minutes after the
157 core was on deck. Under these circumstances, loss of methane due to gas loss was low and methane
158 concentrations could be determined for porewaters that were far above the saturation limit at 1
159 atmosphere pressure for the salinity and temperature range of the bottom water (between 1.9 mM and
160 2.4 mM). A sediment sample of 2.5 mL was taken with a 3 mL cut-off syringe. The sample was
161 transferred to a 20 mL serum vial containing 5 mL 5 M NaCl and immediately closed with a thick
162 septum and an aluminum crimp seal (Thang et al., 2013). For analysis, the sample was shaken and 5
163 mL of brine was injected into a sample vial to displace 5 mL gas out of a vial into the syringe. The CH₄
164 measurements were carried out on a gas chromatograph (GC) with a flame ionization detector (FID)
165 (SRI 8610C) after separation on a 3 feet Porapak Q pre-column before a 9 feet Hayesep D column with
166 N₂ as carrier gas. CH₄ standards 100 ppm, 1000ppm, and 10000 ppm (Air Liquide) were used for
167 calibration.

168 The concentration of methane (mM) of a sample was calculated as follows:

$$169 \quad CH_4(mM) = \frac{CH_{4\ hsp} \cdot V_{hsp}}{1000 \cdot 24.148 \cdot V_{sed} \cdot \rho} \quad (1)$$

170
171 where $CH_{4\ hsp}$ is the concentration of methane in the headspace of the sample vial (ppm), V_{hsp} is the
172 volume of the headspace (L), V_{sed} is the volume of the sediment sample (L), ρ is sediment porosity, and
173 24.148 (L mol⁻¹) is the molar volume of gas at standard pressure 100 kPa and 298 K. The
174 reproducibility of the method has been tested at a station in the archipelago that is not part of this study
175 by replicating methane sampling on multiple sediment cores. Concentrations in multiple cores deviated
176 by about 15%.

177

178 **2.5 Sulfate concentration**

179 Porewater samples for sulfate concentration measurements were obtained using rhizones (Atlas
180 Copco Welltech) (Seeberg-Elverfeldt et al 2005). Rhizones were treated for 2 hours in 2M HCl,

181 followed by two rinses with deionized water for 2 hours and final storage in deionized water. Rhizones
182 were connected to 10 mL disposable plastic syringes via 3-way luerlock stopcocks and inserted in 1-cm
183 intervals through tight-fitting, pre-drilled holes in the liner of the sediment cores. The first mL of pore
184 water was discarded from the syringe. No more than 2 ml were collected from each core to prevent
185 cross-contamination of adjacent intervals (Seeberg-Elverfeldt et al., 2005). Sulfate concentrations were
186 determined with a Dionex System IC 20 ion chromatograph.

187

188 2.6 ³⁵S-Sulfate reduction rates

189 To determine bacterial sulfate reduction rates (SRR) sediment cores were subsampled in 40-cm
190 long 28 mm-diameter cores with 1-cm spaced, silicon-sealed, pre-drilled small holes on the side for
191 injections. For the incubation, the whole-core incubation method by Jørgensen (1978) was used. ³⁵SO₄²⁻
192 tracer solution was diluted in a 6 ‰ NaCl solution containing 0.5 mM SO₄²⁻. 2.5 µl of the tracer
193 solution (50kBq) was injected through the pre-drilled holes. The cores were then capped and sealed in
194 plastic wrap foil and incubated for 8 hours at the respective bottom water temperatures. After this time,
195 the incubations were stopped by sectioning the core in 1-cm intervals to 5 cm depth and in two
196 centimeter intervals below this depth to the bottom of the core. Sediment sections were transferred to
197 50 ml plastic centrifuge tubes containing 20 ml zinc acetate (20% v/v) and shaken vigorously and
198 frozen. The total amount of ³⁵S-labeled reduced sulfur (TRIS) was determined using the single-step
199 cold chromium distillation method by Kallmeyer et al. (2004). TRIS and supernatant sulfate were
200 counted on a TriCarb 2095 Perkin Elmer scintillation counter. The sulfate reduction rate was calculated
201 using the following equation (Jørgensen, 1978):

$$202 \quad {}^{35}SRR = \left(\frac{TRI^{35}S}{({}^{35}SO_4^{2-} + TRI^{35}S)} \right) \cdot 1.06 \cdot SO_4^{2-} \cdot \rho \cdot 1/t \quad (2)$$

203 where SO₄²⁻ is the pore water sulfate concentration corrected for porosity ρ, TRI³⁵S and ³⁵SO₄²⁻ are the
204 measured counts (cpm) of total reduced inorganic sulfur species and sulfate, respectively, 1.06 is a

205 correction factor accounting for the isotope discrimination of ^{35}S against ^{32}S -sulfate, and t is the
206 incubation time. The sulfate reduction rate is reported as $\text{nmol cm}^{-3} \text{ day}^{-1}$. Generally, when enough
207 cores were available ^{35}SRR were measured on replicate cores for all depth intervals. The detection limit
208 of the rate measurements accounting for distillation blanks and radioactive decay of ^{35}S between
209 experiment and laboratory workup was $0.1 \text{ nmol cm}^{-3} \text{ day}^{-1}$.

210

211 **2.7 Whole-core sediment incubations**

212 Four intact cores with undisturbed sediment surfaces and clear overlying water were subsampled in the
213 laboratory in acrylic tubes (i.d. 6.2 cm, height 25 cm) retaining about 10 cm of the overlying water. The
214 sediment height in the tubes was approximately 10 cm. The cores were incubated in a 40-liter
215 incubation tank filled with bottom water from the same station. Before the incubation the overlying
216 water in the cores was equilibrated with bottom water in the tank. The overlying water in the cores was
217 stirred by small magnetic bars mounted in the core liners and driven by an external magnet at 60 rpm.
218 The cores were pre-incubated uncapped for 6 hours and subsequently capped and incubated for a period
219 of 6 to 12 hours depending on the initial oxygen concentration in the bottom water.

220

221 **2.8 Total oxygen uptake**

222 Oxygen sensor spots (Firesting oxygen optode, PyroScience GmbH, Germany) with a sensing surface
223 of 5 mm diameter were attached to the inner wall of two incubation cores (diameter 5.5 cm). The
224 sensor spots were calibrated against O_2 -saturated bottom water and oxygen-free water following the
225 manufacturer's guidelines accounting for temperature and salinity of the incubation water.
226 Measurements were performed with a fiberoptic cable connected to a spot adapter fixed at the outer
227 core liner wall at the spot position. The O_2 concentration was continuously logged during incubations.

228 Sediment total oxygen uptake (TOU) rates were computed by linear regression of the O₂ concentration
229 over time.

230

231 **2.9 Methane fluxes**

232 Methane fluxes were determined from discrete water samples collected without headspace in 12 mL
233 Exetainers (Labco, Wycombe, UK) prefilled with 50 µL of 50% ZnCl₂. Samples were collected at the
234 beginning (time zero) and the end of the incubation (time final), usually after 24 hours. CH₄
235 concentrations were determined using the headspace equilibration technique (Kampbell et al., 1989) by
236 replacing 3 ml of the water in the exetainers with high-purity helium gas at atmospheric pressure. The
237 Exetainers were then shaken at 400rpm on a shaking table for 60 minutes to allow the gas to equilibrate
238 between the headspace and the liquid phase and left to rest for half an hour. After equilibration 2.5 mL
239 of NaCl brine was injected into an Exetainer to force the gas samples into an injection syringe while
240 maintaining the headspace pressure. The samples were injected onto a 1 ml injection loop of a gas
241 chromatograph (SRI 8610C) with FID detector using N₂ as carrier gas. CH₄ standards 5 ppm, 100 ppm
242 and 1000 ppm (Air Liquide) were used to construct a calibration curve. The partial pressure of CH₄ in
243 the equilibrated headspace and water was calculated using the solubility coefficient β for CH₄ using the
244 salinity of the bottom water at the respective sample time (Table 1) (Wilhelm et al 1977), gas constant
245 R (8.314 L kPa mol⁻¹ K⁻¹), air pressure P (kPa), headspace gas concentration CH_{4 hsp} (nmol), headspace
246 volume (0.003L), water volume in the exetainer (0.009L), and laboratory temperature T (293 K)
247 according to

$$248 \text{CH}_4 \text{ (nM)} = (\text{CH}_4 \text{ hsp} + \beta \text{CH}_4 \text{ hsp}) * P/RT \quad (3)$$

249 Fluxes (J) of CH₄ (mmol m⁻² d⁻¹) during the whole core sediment incubations were calculated according
250 to

$$251 J = (\text{CH}_4 \text{ start} - \text{CH}_4 \text{ end})/t * V/A \quad (4)$$

252 where $\text{CH}_4_{\text{start}}$ and $\text{CH}_4_{\text{final}}$ represent the end and start concentrations in mmol/m^3 , V is headspace
253 volume (m^3), A is the surface area of the incubation core (m^2), and t is the incubation time (days).

254

255 **2.10 Diffusive flux calculations**

256 Diffusive fluxes of methane and sulfate were estimated from the porewater gradients of methane and
257 sulfate for the sediment surface and the sulfate-methane transition zone. Sediment cores at station B1
258 showed occasional burrows from deposit feeders in the topmost 2 cm of sediment, whereas sediment at
259 station H6 was largely devoid of macro- and meiofauna. Since only one sample was taken from the
260 topmost 2 cm, quantitative depth-related effects of bioturbation cannot be accounted for in this analysis
261 and upward diffusive transport of methane was assumed as the dominant transport pathway. Fluxes
262 were estimated using Fick's first law of diffusion

$$263 \quad J = D_s \frac{dC}{dx} \quad (5)$$

264 assuming that flux was dominated by molecular diffusion, where dC is the change in concentration of
265 dissolved sulfate (mM) or methane (mM) over a depth interval dx (cm), and D_s is the sediment
266 diffusion coefficient calculated for the bottom water temperature and salinity according to Boudreau
267 (1996). D_s was recalculated from the molecular diffusion coefficient D_o for sulfate and methane
268 according to Iversen and Jørgensen (1994). Since the resolution of the porewater methane analysis was
269 2 cm, concentration changes below this resolution cannot be resolved. This could lead to an
270 overestimation of the flux across the sediment surface, e.g., due to aerobic methane oxidation in the
271 topmost mm of sediment. Similar effects may occur in the sulfate-methane transition zone.

272

273 **3 Results**

274 **3.1 Bottom water temperature, dissolved oxygen, sediment organic carbon**

275 Over the observation period April 2012 through February 2013 bottom water salinity varied between
276 6.5 and 7.0‰ at station B1 and 5.4 and 6.5‰ at Station H6 (Table 1), while bottom water temperatures
277 ranged from 2.4°C to 6.9°C for station B1 and 1.8°C to 9.4°C for station H6. The lowest and highest
278 bottom water oxygen concentrations measured were 160 µM for station B1 and 40 µM for station H6 in
279 April 2012, and 300 µM and 380 µM for station B1 and station H6 in February 2013, respectively.
280 Surface sediment organic carbon concentrations were similar at the two stations ranging between 4.6
281 and 5.2% at Station B1, and 5.0% and 6.0% at Station H6 over the observation period.

282

283 **3.2 Methane and sulfate concentrations**

284 At both stations, the measured methane concentrations never exceeded the solubility limit for methane
285 calculated for the *in situ* pressure, which ranged from 9.6 to 11.9 mM during the different sampling
286 periods. At station B1, the highest methane concentrations in the sediment cores were recorded in
287 October 2012, when they reached 0.9 mM (Figure 2a-d). Surprisingly, the lowest methane
288 concentrations were recorded in August 2012. This was possibly due to drift of the vessel during
289 sampling in rough seas at that time into an area underlain by neighbouring glacial clays with low
290 porewater methane concentrations. Excluding the August data, methane concentrations were low and
291 between 1 and 10 µM to a depth of 6 cm, 2 cm, and 6 cm in April, October, and February, respectively,
292 before they increased sharply. At station H6, the highest and lowest concentrations in the cored depth
293 interval were 5.7 mM and 1.5 mM, and recorded in August and February 2013, respectively. At this
294 station, the methane concentrations generally increased linearly from the surface down to 10 cm depth.
295 Below this depth they only increased slightly or remained constant.

296 Sulfate concentration gradients changed between the different seasons at both stations reflecting
297 changes in sulfate reduction rates over the observation period. At both stations, the sulfate

298 concentration gradients were steepest in the topmost 8-10 cm in August, intermediate in April and
299 October, and lowest in February indicating highest and lowest sulfate reduction rates in late summer
300 and winter, respectively (Figure 2 a-h). At station B1, sulfate was never consumed completely and
301 concentrations remained above 1.5 mM at the bottom of the core. In August and October, a distinct
302 decrease in the sulfate concentration gradient occurred at around 8-10 cm depth. Despite some
303 variability in the sulfate concentration profiles, the sulfate concentrations at the bottom of the core were
304 similar during all observation periods. At station H6, sulfate always reached minimum concentrations
305 of less than 100 μM in the cored sediment interval, albeit at substantially greater depth in February.
306 The initial depth at which sulfate reached the lowest concentration from the surface down was defined
307 as the initial minimum sulfate concentration depth, which occurred at 16 cm depth in April, 10 cm in
308 August, 14 cm in October and at 25 cm depth in February.

309

310 **3.3 ^{35}S -sulfate reduction rates**

311 At Station B1, the depth-integrated SRR over the cored depth varied from 0.5 to 2.3 $\text{mmol m}^2 \text{d}^{-1}$. The
312 depth-resolved SRR ranged from 63 $\text{nmol cm}^{-3} \text{d}^{-1}$ at the sediment surface to 0.2 $\text{nmol cm}^{-3} \text{d}^{-1}$ at the
313 bottom of the cored intervals (Figure 3 a-h, Table 2). Contrary to expectations, the lowest SRR were
314 measured in August, which was possibly also due to the fact that the vessel drifted into a glacial clay
315 area. The highest SRR were measured in the topmost 2 cm with the exception of October 2012, when
316 the maximum was found at 3 cm depth. Below the depth of maximum SRR, rates decreased
317 exponentially indicating that organoclastic sulfate reduction dominated and that the reactivity of the
318 degrading organic material decreased exponentially with depth. More than 90% of the integrated
319 sulfate reduction took place in the top 15 cm of sediment (Figure 5 a-d). Over the cored sediment
320 interval, there was no peak that could be attributed to significant AOM. Nevertheless, the distinct
321 curvature of the methane concentration profile in February 2013 at station B1 suggests that methane
322 was oxidized in the sulfate reduction zone and that some of the sulfate reduction may have been
323 coupled to anaerobic methane oxidation.

324 At Station H6, depth-integrated SRR varied 9.2 to 11.7 mmol m⁻² d⁻¹. The highest measured SRR was
325 338 nmol cm⁻³ d⁻¹ and occurred at 2 cm depth in April 2012. Organoclastic sulfate reduction dominated
326 the interval down to 10 cm. In April, August, and October 2012 two distinct sulfate reduction rate
327 peaks were found at station H6, one at the surface, and a second peak between 10 cm and 18 cm depth.
328 The latter peak covers the sulfate-methane transition zone and indicates that in this depth interval the
329 rates of anaerobic methane oxidation coupled to sulfate reduction exceeded organoclastic sulfate
330 reduction rates. We therefore defined the depth interval near the minimum sulfate concentration depth
331 together with elevated SRR as the AOM zone (Table 2). Previous studies at nearby station H5 in
332 Himmerfjärden also found AOM to be present at depths between 6 and 16 cm, which is in agreement
333 with our findings (Thang et al., 2013; Wegener et al., 2012). The depth-integrated rates of SRR in the
334 sulfate-methane transition zone at H6 were relatively constant over the three observation periods and
335 varied between 2.4 mmol m⁻² d⁻¹ and 2.8 mmol m² d⁻¹ (Table 2). In February, however, when sulfate
336 penetrated to 24 cm depth, sulfate reduction rates were about two times lower compared to the other
337 months. The previously observed elevated rates between 10 and 18 cm depth were not visible, although
338 another SRR peak was observed between 5 and 9 cm depth. However, the high concentrations of
339 sulfate and low concentrations of methane in this depth interval in February make it unlikely that this
340 peak is due to AOM. It is more likely that this peak is associated with organoclastic sulfate reduction,
341 because no change in the sulfate or methane gradients was observed at this depth. Some sulfate
342 reduction was also detected below 18 cm depth at station H6 in April, August, and October. Since non-
343 radioactive carrier sulfate was added to the ³⁵S-tracer during these incubations, these rates indicate
344 potential sulfate reduction activity in the methanogenic zone (Leloup et al., 2009).

345 346 **3.4 Benthic exchange of oxygen, sulfate, and methane**

347 Rates of total oxygen uptake are summarized in Table 2 and shown for comparison in Figure 4. Total
348 oxygen uptake was lowest in February at both stations (B1: 12.0 ± 1.5 mmol m⁻² d⁻¹ and H6: 14.9 ± 1.6
349 mmol m⁻² d⁻¹), and highest in August at station B1 (22.5 ± 2.9 mmol m⁻² d⁻¹) and in April at station H6

350 $(33.5 \pm 3.5 \text{ mmol m}^{-2} \text{ d}^{-1})$. Diffusive fluxes of sulfate from the water column into the sediment ranged
351 from $0.2 \text{ mmol m}^{-2} \text{ d}^{-1}$ in February to $1.4 \text{ mmol m}^{-2} \text{ d}^{-1}$ in October at station B1, and from 1.3 mmol m^{-2}
352 d^{-1} in February to $2.7 \text{ mmol m}^{-2} \text{ d}^{-1}$ in August at station H6 (Table 2). These rates are significantly
353 lower than the depth-integrated radiotracer rates and indicate that sulfate is reoxidized below the
354 sediment surface by reaction with reactive iron (Thang et al., 2013). Whole-core methane fluxes ranged
355 from $-0.1 \pm 0.05 \text{ mmol m}^{-2} \text{ d}^{-1}$ (February) to $-1.2 \pm 0.6 \text{ mmol m}^{-2} \text{ d}^{-1}$ (August) at station B1 and from -
356 $0.3 \pm 0.1 \text{ mmol m}^{-2} \text{ d}^{-1}$ (April 2012) to $-19.9 \pm 7.8 \text{ mmol m}^{-2} \text{ d}^{-1}$ (August) at station H6 (Figure 5, Table
357 2). However, the following year, a significantly higher methane flux of $3.9 \text{ mmol m}^{-2} \text{ d}^{-1}$ was measured
358 in April 2013 at station H6. Significant upward diffusive methane fluxes ranged from $0.02 \text{ mmol m}^{-2} \text{ d}^{-1}$
359 d^{-1} (February 2012) to $0.3 \text{ mmol m}^{-2} \text{ d}^{-1}$ (August) at Station B1 and from 0.5 (February) to 2.3 mmol m^{-2}
360 d^{-1} (August) at station H6. Thus, there was a generally poor agreement between whole-core and
361 diffusive flux-derived methane fluxes. The large discrepancy between the August 2012 diffusive flux
362 and whole-core flux is best explained that the cores were taken from sediments with different organic
363 carbon contents. Since several Multicorer casts were taken per station and the vessel's positioning
364 ability in strong winds was at best tens of meters, sediment heterogeneity can possibly explain this
365 difference. The very high whole-core flux value measured in August 2012 at Station H6 is likely due to
366 ebullition during the incubation at ambient air pressure and oversaturation of the porewater with respect
367 to atmospheric pressure.

368

369 **4. Discussion**

370 **4.1 Bottom water temperature and salinity**

371 Correlations between biogeochemical rates and fluxes with bottom water temperatures in
372 Himmerfjärden between April 2012 and February 2013 were weak for the period April-October, and
373 forced by the low rates in the coldest observation period in early February 2013. All R values
374 calculated for pairs of temperature versus rate/flux were less than 0.2 and not consistent for the fluxes

375 of oxygen, methane, and sulfate indicating that additional environmental controlling factors played a
376 role. It is likely that the microbial community involved in the cycling of methane and sulfur species in
377 Himmerfjärden sediment is temperature-sensitive, and that the low rates in February 2013 are due to
378 the 3°C temperature drop in bottom water from October 2012 to February 2013 (Table 1). This would
379 be consistent with rate observations in comparable environments by Treude et al (2005a), Abril and
380 Iversen (2002), Crill and Martens (1983), and Westrich and Berner (1988), and is also supported by
381 studies of the microbial community composition of estuarine sediments that showed variations as a
382 function of temperature (e.g., Zhang et al 2014). Regulation of methane fluxes largely by temperature
383 implies that methane oxidation in Himmerfjärden sediment is less temperature-sensitive than
384 methanogenesis preventing methane oxidizing bacteria from keeping up with the enhanced methane
385 flux during summer. This requires significantly higher temperature stimulation of methanogenesis than
386 methane oxidation, the lack of an electron acceptor, or competition for the same electron acceptor used
387 by other organisms than methane-oxidizing bacteria. Publications from lake environments and
388 terrestrial environments suggest that aerobic methane-oxidizing bacteria may indeed be less
389 temperature-sensitive than methanogens (King, 1992; Wik et al., 2014; Nguyen et al., 2011). However,
390 this argument is not directly applicable to marine habitats. In case of anaerobic methane oxidation, it is
391 difficult to argue for a physiological temperature disadvantage of methane oxidizers compared to
392 methanogens, because of the tight coupling between sulfate reduction and methane oxidation, the
393 phylogenetic proximity of ANME to known methanogenic Archaea (Knittel and Boetius, 2009), and
394 similarities in membrane composition of ANME and methanogenic Archaea (Wegener et al., 2012).
395 However, temperature control may not manifest itself by direct kinetic or bioenergetic regulation, but
396 indirectly through the influence on competing processes, e.g., sulfate reduction and methanogenesis.
397 Further, microbial community composition and biogeochemical rates often cannot be directly
398 established from binary relationships with temperature, since other physical and chemical parameters
399 such as salinity, bottom water oxygen concentrations, organic carbon accumulation also vary
400 seasonally. Of these, salinity is not considered to be important for the present study, because the annual

401 range in Himmerfjärden bottom water was only between 5.4 and 7 ‰, which is too small to affect the
402 major electron acceptor and carbon degradation pathways.

403

404 **4.2 Effects of organic matter composition and sedimentation**

405 Organic carbon concentrations in Himmerfjärden are comparable to other fjord- and fjärd-type
406 estuarine sediments (Bianchi, 2007; Smith et al., 2015). Primary organic carbon export in
407 Himmerfjärden varies strongly on both seasonal and interannual timescales (Blomqvist and Larsson,
408 1994). The major export periods occur during the spring phytoplankton bloom after ice breakup from
409 March-April until early May, during a late-summer cyanobacterial bloom in August, and after a
410 weaker, secondary phytoplankton bloom in September (Bianchi et al., 2002; Zakrisson et al., 2014;
411 Harvey et al., 2015). Terrestrial-derived organic carbon that is not derived from the sewage treatment
412 plant plays only a minor role in this system, because no major rivers enter the system and surface
413 rainwater runoff is low. Based on sediment trap studies, the annual organic carbon flux in
414 Himmerfjärden varies by more than an order of magnitude at station B1 and by about a factor of 3 in
415 the inner parts of Himmerfjärden (Blomqvist and Larsson, 1994). Observations over a 5-year period by
416 Blomqvist and Larsson (1994) indicated that primary organic carbon dominates organic sedimentation
417 in the spring and summer at station B1, whereas station H6 is characterized by a spring term dominance
418 of primary carbon deposition, but a much greater contribution of resuspended organic material to
419 organic sedimentation during the fall (Blomqvist and Larsson, 1994).

420 A second effect to be considered is that stations B1 and H6 are located in bathymetric depressions. H6
421 is in the center of a sub-basin separated from the outer Himmerfjärd by a sill (Fig. 1). Likewise, Station
422 B1 is located in a small depression at the head of a submarine channel that opens to the Baltic Sea.
423 Fine-grained and reworked organic-rich material preferentially accumulates in these depressions
424 (Jonsson et al., 2003). Because of the importance of resuspended organic material for the vertical mass
425 flux and bioturbation, the annual variability in the organic matter composition at the sediment surface
426 varies year-round only between 5 and 6 % OC with relatively constant C/N ratios between 7.9 and 9.1

427 at Station B1 and 8.3 and 9.2 at Station H6 (Bonaglia et al., 2014). Organic mass accumulation rates in
428 the accumulation bottoms based on ^{210}Pb dating are reported between 3.3 and 9.5 mol m⁻² y⁻¹ (Thang et
429 al., 2013; Karlsson et al., 2010). The combined effect of these sedimentation characteristics is that
430 temporal variability in the settling primary organic carbon flux above the sediment surface is low,
431 which reduces the overall temporal variability in organic carbon amount and composition and thereby
432 in carbon mineralization rates. This small temporal variability is further influenced by macrofauna
433 bioturbation in the top 2-3 cm of sediment in this area, foremost by the bivalve *Macoma baltica*, the
434 arthropod *Pontoporeia femorata*, and the polychaete *Marenzelleria* (Bonaglia et al., 2014). Although
435 macrofauna is largely absent at Station H6, sediment is also mixed at station H6 by bioturbating
436 meiofauna (mostly ostracods) (Bonaglia et al., 2014).

437 The measured benthic oxygen uptake rates are consistent with the low variability in the surface organic
438 carbon concentrations, C/N ratios, and a temperature-dependent decrease in total oxygen uptake rates in
439 winter. The slightly higher total oxygen uptake rate at Station H6 is also consistent with the
440 physiography of the enclosed small basin favouring sediment trapping of fine material. In addition, the
441 location of station H6 in the inner fjärd limits water exchange and leads to greater oxygen depletion,
442 whereas the more open station B1 is affected by upwelling of oxygen-rich waters and comparatively
443 less burial of organic material (Table 1).

444

445 **4.3 Methane fluxes, sulfate reduction and methane oxidation**

446 Sediment focusing in the sub-basins of the inner Himmerfjärden sediments results in very high
447 sedimentation rates between 0.9 and 1.3 cm/yr (Thang et al., 2013; Bianchi et al., 2002). In such
448 sediments organic carbon burial and transfer of organic matter into the methanogenic zone is efficient
449 and will occur within 20 to 30 years. As a consequence of the low bottom water salinity of 6 ‰ of the
450 Baltic Sea at this latitude, seawater sulfate concentrations are less than 7 mM and, by comparison with
451 normal seawater, a comparatively lesser amount of organic matter can be degraded by bacterial sulfate
452 reduction (Thang et al., 2013). Consequently, compared to normal marine sediments a larger proportion

453 of organic matter undergoes anaerobic microbial degradation terminating in methanogenesis, which
454 generates a high upward flux of methane into the sulfate-containing zone. Organoclastic sulfate-
455 reducing bacteria will compete for the available sulfate with sulfate-reducing bacteria involved in the
456 anaerobic oxidation of methane (Dale et al., 2006; Jørgensen and Parkes, 2010). Thermodynamic and
457 kinetic constraints decide on the outcome between these two competing processes. Dale et al. (2006)
458 suggested that due to lower winter temperatures and greater sulfate availability in the sulfate-methane
459 transition zone in winter, the thermodynamic driving force for anaerobic methane oxidation increases
460 allowing for a greater proportion of anaerobic methane oxidation coupled to sulfate reduction in the
461 winter. In the summer and fall, higher temperatures and sulfate limitation may favor organoclastic
462 sulfate reduction and methanogenesis while limiting the anaerobic oxidation of methane. Most
463 importantly, however, their analysis showed that due to thermodynamic constraints and slow growth
464 rates of the methane-oxidizing archaea the microbial biomass does not change significantly over a year.
465 These conceptual modelling results can be tested with our Himmerfjärden data.

466 Sulfate reduction rates, particularly at H6, demonstrate how strongly bottom-water oxygen controls
467 organic matter mineralization. In the spring, summer, and fall sulfate reduction was at its maximum in
468 the first two centimeters of the sediments (Fig 3 e, f, g). In February, reduced organic carbon input and
469 higher oxygen concentrations resulted in lower sulfate reduction rates and a shift of the maximum rates
470 to greater depths in the sediment confining methane production to greater depths in the sediment.

471 The decrease in oxygen uptake matches well with the decrease in methane fluxes at the two stations in
472 winter, which suggests an impact of oxygen on methane cycling (Table 2, Figure 5). Higher oxygen
473 levels enhance bioturbation and oxygen uptake by the abundant macro- and meiofauna (Norkko et al.,
474 2015), but the mixing of sediment also affects methane transport to the water column, as the main
475 transport process shifts from diffusion to advection. This effect is likely the main cause for the winter
476 decrease in methane fluxes and concentrations. More aerated conditions indirectly enhance methane
477 removal by sustaining aerobic methanotrophs (Valentine 2011). It is plausible that, as in other brackish
478 coastal sediments, aerobic methanotrophs at the surface of Himmerfjärden sediments consume a

479 significant part of upward-diffusing methane that was not oxidized by anaerobic methane oxidation
480 (McDonald et al 2005, Moussard et al 2009, Treude et al 2005a).

481 Published benthic methane fluxes for estuaries with similar salinities have a reported range of 0.002 to
482 0.25 mmol m⁻² d⁻¹ (Abril and Iversen, 2002; Martens and Klump, 1980; Sansone et al., 1998; Zhang et
483 al., 2008; Borges and April, 2012; Martens et al., 1998). The methane fluxes derived from our core
484 incubations (0.1-3.9 mmol m⁻² d⁻¹, ignoring the potentially biased value of 19.9 mmol m⁻² d⁻¹) and the
485 corresponding diffusive fluxes (0.01-2.4 mmol m⁻² d⁻¹) were high compared to these published fluxes.
486 However, our fluxes are consistent with fluxes based on porewater gradients by Thang et al. (2013) that
487 were between 0.3 and 1.1 mmol m⁻² d⁻¹ at 3 nearby stations measured in May 2009.

488 A conspicuous property of all porewater profiles at station H6, with the exception of the February 2013
489 sampling period, was the absence of a curvature in the methane concentration profiles, which would be
490 expected for net methane oxidation by aerobic and anaerobic methane oxidation (Martens et al., 1998).
491 Most concentration profiles of sulfate and methane at Station H6 overlapped without a significant
492 change in the methane concentration gradient. A similar observation has been made earlier for other
493 Himmerfjärden sediments (Thang et al., 2013), and has also been reported for sediments of the
494 northwestern Black Sea shelf (Knab et al., 2009) and in organic-rich shelf sediment of the Namibian
495 upwelling system (Brüchert et al., 2009). Inefficient methane oxidation is also evident from the
496 diffusive fluxes, which showed that the upward fluxes of methane into the sulfate-methane transition
497 zone were only marginally higher than the methane fluxes to the sediment surface indicating little
498 attenuation of the methane flux in the sulfate-methane transition zone (Table 2). One possible
499 explanation for this phenomenon is therefore that rates of sulfate reduction-coupled anaerobic methane
500 oxidation, except for the winter months, were low compared to the total sulfate reduction rate. An
501 alternative explanation of our observations could be that the methane concentration gradients were
502 affected by the presence of rising methane bubbles (Haeckel et al., 2007), or that bioturbation and
503 bioirrigation linearized the concentration profiles (Dale et al., 2013). However, we do not favor these
504 latter interpretations because of the absence of large macrofauna at station H6, the fact that methane

505 concentrations were below the in-situ saturation concentration of methane, and the fast porewater
506 methane sampling method preventing significant gas formation.

507 An analysis of the cumulative distribution of ^{35}S -SRR with depth at station H6 provides clues to the
508 proportion of organoclastic relative to anaerobic methane oxidation-coupled sulfate reduction at Station
509 H6 (Figure 6 e-h). In contrast to station B1, where an exponentially decreasing portion of sulfate
510 reduction contributed to the total sulfate reduction at depth, at station H6 a distinct steepening in the
511 cumulative sulfate reduction is observed below 10 cm in April, August, and October. As discussed
512 above, we do not attribute the steepening observed in February 2013 to the same process, because
513 sulfate was still present in abundance at this depth and methane concentrations were low and without
514 any apparent change in gradient in this depth zone. The gradient in organoclastic sulfate reduction can
515 be described by an exponential function (Jørgensen and Parkes, 2010),

$$516 \quad {}^{35}\text{SRR} = y z^{-b} \quad (6)$$

517 where z is depth (cm) and y and b are regression coefficients (Jørgensen and Parkes, 2010). Fitting the
518 sulfate reduction rates investigated here to such a function yielded exponential coefficients b between
519 0.4 and 0.9 at station B1 and 0.3 and 0.8 at Station H6 (Table 4). At Station H6 the lowest coefficient
520 was found for February 2013, when sulfate penetrated the deepest into the sediment (Table 4). Since
521 the upward flux of methane provides an additional energy source to sulfate-reducing bacteria, total
522 sulfate reduction rates are expected to increase in the sulfate-methane transition zone. If substantial
523 AOM-coupled and organoclastic sulfate reduction occur at the same depths the total ^{35}S -sulfate
524 reduction rate depth gradient will be lower and the exponential coefficient b will be smaller than for a
525 setting without significant AOM. The difference between the exponential coefficients for the different
526 observation times can be used to calculate the variation in the contribution of AOM to the total sulfate
527 reduction rate. At station H6, between 5 % (August 2012) and 20% (April 2012) of the total sulfate
528 reduction can be associated with anaerobic methane oxidation. A comparison of the above method with
529 the ^{35}S -sulfate reduction rates integrated over the length of the H6 sediment cores with the rates
530 integrated in the AOM zone also indicated that >20% of sulfate reduction at H6 was supported by

531 anaerobic methane oxidation (Table 2). In near-shore continental margin sediments worldwide, the
532 fraction of methane-driven sulfate reduction varies between locations and accounts for 3-40% of total
533 sulfate reduction, with 10% possibly representing a global mean value (Jørgensen and Kasten, 2006).
534 The average 20% contribution calculated here falls in the upper range of these values and is similar to
535 values reported before for one of the monitoring stations within Himmerfjärden (Thang et al., 2013)
536 and also for a very productive Chilean slope sediment (8-24 %) (Treude et al 2005b). The good match
537 between the upward fluxes of methane in the sulfate-methane transition zone and the measured sulfate
538 reduction rates in the transition zone also indicate that other proposed electron acceptors for anaerobic
539 methane oxidation such as iron are unimportant in these sediments (Beal et al., 2009; Egger et al.
540 2014).

541

542 **4.4 Temporal variability in hydrostatic pressure**

543 The abrupt decrease in porewater methane concentrations from October 2012 to early February 2013
544 and the subsequent increase in April 2013 cannot be explained by variation in methane oxidation alone,
545 because the temporal change in porewater methane concentration was large compared to the inferred
546 methane oxidation rates based on fluxes in and out of the AOM zone. In addition, except for
547 downward-diffusing sulfate, there was no significant other electron acceptor present at depth. It is
548 unlikely that rates of methanogenesis would have decreased significantly between the fall and the
549 winter and resumed again in the spring because of the sedimentological characteristics described above
550 and the small difference in sediment temperatures for February and April (Table 1). Changes in organic
551 matter sedimentation at the sediment surface also have no significant influence on methanogenesis rates
552 in buried sediment and cannot explain the sudden decrease in methane concentration at depth. An
553 alternative explanation for the changes in methane concentrations is required. A possible explanation
554 could be that changes in upward transport of methane are due to variability in hydrostatic pressure and
555 the associated diffusive and advective upward transport of methane from depth. The free gas depth of
556 methane is thought to follow changes in hydrostatic pressure and temperature (Mogollon et al., 2011;

557 Toth et al., 2015). An estimated 10% of the fine-grained sediments in the Stockholm archipelago area
558 are underlain by pockets of free methane (Persson and Jonsson, 2000) and these free gas pockets are
559 preferentially located in areas with the thickest postglacial mud accumulation, generally in the center of
560 the sub-basins and along fault lineaments (Söderberg and Floden, 1992). Based on sub-bottom
561 echosounder profiling, the surface of the free gas zone in accumulation areas in Himmerfjärden and
562 other areas of the Stockholm archipelago is between 1 and 3 meter depth (Söderberg and Floden,
563 1991). During low sealevel stand the free gas zone is expected to migrate closer to the sediment
564 surface, whereas during high sealevel the free gas zone is depressed into the sediment. The total
565 variation in sealevel is related to air pressure, prevailing wind directions, precipitation, and the balance
566 of saltwater entry through the Danish straits and freshwater discharge from rivers entering the Baltic
567 Sea (Andersson, 2002). Additional effects are caused by local coastal bathymetry, current flow, and,
568 possibly, and local submarine groundwater discharge. These multiple parameters result in complex
569 subsurface hydrology and may produce sealevel fluctuations that can be as much as 50 cm, sufficient to
570 explain the changes in methane concentrations observed here. Unfortunately, local data within
571 Himmerfjärden on sealevel fluctuations are not available for our respective sampling locations, and
572 regional sealevel stands should not be directly applied to the sample sites.

573 The above discussion demonstrates that a variety of processes interact in these fjord sediments to
574 produce the observed methane fluxes. It is beyond the scope of this paper to develop a unifying model
575 against which the variability of the observed fluxes can be tested, but we would like to point out that
576 the local coastal hydrography and hydrogeology would need to be accounted for in such a coupled
577 physical biogeochemical model. To our knowledge, sufficient subsurface geophysical data are currently
578 not available to establish appropriate physical boundary conditions for such a model. Detailed
579 geophysical analysis of the subsurface structure at high vertical resolution together with long-term
580 monitoring of the porewater chemistry would shed new light on the coupling between subsurface
581 hydrology and methane emissions.

582

583

584 **5 Conclusions**

585 A greater understanding of methane emissions from estuarine and coastal sediments is important to
586 estimate the contribution of these environments to global marine methane fluxes. High benthic fluxes
587 of methane from these sediments showed that total methane oxidation was relatively inefficient, despite
588 the fact that anaerobic methane oxidation contributed up to 20% to total sulfate reduction. Of the
589 different environmental regulators, bottom water oxygen had the strongest influence for the regulation
590 of methane emissions. Oxygen availability directly enhanced aerobic organic matter mineralization by
591 shifting the redox cascade in the sediments and indirectly by stimulating meiofauna and macrofauna
592 activity thereby stimulating both the aerobic carbon mineralization and oxidative recycling of sulfate.
593 The annual variability in sediment methane concentrations and benthic methane fluxes indicate that the
594 annual environmental changes at these near-shore, but relatively deep-water localities are considerable.
595 Very few data on sediment biogeochemical processes are currently available for aerobic and anaerobic
596 carbon mineralization and methane cycling during winter months when ice cover inhibits access and
597 sampling. Process rates inferred from sampling during open-water conditions over the whole year are
598 therefore likely overestimates.

599 Hydrostatic pressure changes and complex subsurface hydrological conditions may also affect the
600 temporal variability of subsurface methane concentrations. The spatial and temporal variability of these
601 conditions must also be considered as an important component for understanding methane emissions
602 from near-shore coastal and estuarine waters.

603

604

605 **6. Author contribution**

606 Joanna E. Sawicka conducted the sampling and analysis for the study and wrote the manuscript. Volker
607 Brüchert devised the study, interpreted the data, created the figures and tables, and wrote the
608 manuscript.

609

610 **7. Data availability**

611 The data are available from the second author upon request.

612

613 **8. Acknowledgments**

614 We are grateful to the staff of Askö Laboratory for their help and cooperation during the cruises and
615 our stays on the island of Askö. We would like to thank Barbara Deutsch, Camilla Olsson and Stefano
616 Bonaglia for their help during sampling. The study was funded by the grant from the Bolin Centre for
617 Climate Research, Baltic Ecosystem Adaptive management (BEAM), and the EU BONUS project
618 Baltic Gas. We acknowledge the comments by two reviewers that substantially changed the
619 manuscript.

620

621 **References**

- 622 Abril, G. and Iversen, N.: Methane dynamics in a shallow non-tidal estuary (Randers Fjord, Denmark), *Mar Ecol Prog Ser*,
623 230, 171-181, 2002.
- 624 Amouroux, D., Roberts, G., Rapsomanikis, S. and Andreae, M.O.: Biogenic gas (CH₄, N₂O, DMS) emission to the
625 atmosphere from near-shore and shelf waters of the North-western Black Sea, *Estuar Coast Shelf S*, 54, 575-587,
626 2002.
- 627 Bange, H. W., Bergmann, K., Hansen, H. P., Kock, A., Koppe, R., Malien, F., Ostrau, F., Dissolved methane during hypoxic
628 events at the Boknis Eck time series station (Eckernförde Bay, SW Baltic Sea), *Biogeosciences*, 7, 1279-1284,
629 2010.
- 630 Beal, E. J., House, C. H., Orphan, V. J.: Manganese- and Iron-Dependent Marine Methane Oxidation, *Science* 325, 184-
631 187, 2009.
- 632 Bianchi, T. S., Engelhaupt, E., McKee B. A., Miles, S., Elmgren, R., Hajdu, S., Savage, C., and Baskaran, M.: Do sediments
633 from coastal sites accurately reflect time trends in water column phytoplankton? A test from Himmerfjärden Bay
634 (Baltic Sea proper), *Limnol. Oceanogr.*, 47, 1537-1544, 2002.
- 635 Blomqvist, S. and Larsson, U.: Detrital bedrock elements as tracers of settling resuspended particulate matter in a coastal
636 area of the Baltic Sea, *Limnol. Oceanogr.*, 39, 880-896, 1994.
- 637 Boesch, D. F., Hecky, R., O'Melia, C., Schindler, D., Seitzinger, S.: Eutrophication of the Swedish Seas, Reports of the
638 Swedish Environmental Protection Agency, Stockholm, Sweden, No. 5509, 72 p, 2006.
- 639 Bonaglia, S., Bartoli, M., Gunnarsson, J. S., Rahm, L., Raymond, C., Svensson, O., Shakeri, Brüchert, V.: Effect of
640 reoxygenation and *Marenzelleria* spp. bioturbation on Baltic Sea sediment metabolism, *Marine Ecology Progress*
641 *Series*, 482, 43-55, 2013.
- 642 Bonaglia, S., Deutsch, B., Bartoli, M., Marchant, H. K. and Brüchert, V.: Seasonal oxygen, nitrogen and phosphorus benthic
643 cycling along an impacted Baltic Sea estuary: regulation and spatial patterns, *Biogeochemistry*, 119, 1-22, 2014.
- 644 Borges, A. V. and Abril, G.: Carbon Dioxide and Methane Dynamics in Estuaries, in: *Treatise on Estuarine and Coastal*
645 *Science*, (Eds.) Wolanski, E., McLusky, D., Academic Press, Waltham, 119-161, 2011.
- 646 Boudreau, B.P.: *Diagenetic models and their implementation*. Springer Verlag, Berlin Heidelberg, 1996.
- 647 Brüchert, V., Currie, B., Peard, K.: Hydrogen sulphide and methane emissions on the central Namibian shelf, *Progr.*
648 *Oceanogr.*, 83, 169-179, 2009.
- 649 Crill, P. M. and Martens, C. S.: Spatial and temporal fluctuations of methane production in anoxic coastal marine sediments,
650 *Limnol. Oceanogr.*, 6, 1117-1130, 1983.
- 651 Dale, A. W., Regnier, P., Van Cappellen, P.: Bioenergetic Controls on Anaerobic Oxidation of Methane (AOM) in Coastal
652 Marine Sediments: A Theoretical Analysis, *Am. J. Sci.*, 306, 246-294, 2006.
- 653 Dale, A. W., Aguilera, D. R., Regnier, P., Fossing, H., Knab, N. J., Jørgensen, B. B.: Seasonal dynamics of the depth and
654 rate of anaerobic oxidation of methane in Aarhus Bay (Denmark) sediments, *J. Mar. Res.*, 66, 127-155, 2008.
- 655 Dale, A. W., Bertics, V. J., Treude, T., Sommer, S., Wallmann, K.: Modeling benthic-pelagic nutrient exchange processes
656 and porewater distributions in a seasonally hypoxic sediment: evidence for massive phosphate release by
657 *Beggiatoa*? *Biogeosciences*, 10, 629-651, 2013.
- 658 Egger, M., Rasigraf, O., Sapart, C. J., Jilbert, T., Jetten, M. S. M., Röckmann, T.: Iron-mediated anaerobic oxidation of
659 methane in brackish coastal sediments, *Env. Sci. Technol.*, 49, 277-283, 2014.
- 660 Elmgren, R. and Larsson, U.: Himmerfjärden: förändringar i ett näringsbelastat kustekosystem i Östersjön, Reports of the
661 Swedish Environmental Protection Agency, Stockholm, Sweden, 1997.
- 662 Engqvist, A., Long-term nutrient balances in the eutrophication of the Himmerfjärden, *Estuar. Coast. Shelf S.*, 42, 483-507,
663 1996.
- 664 Giuseppe Etiope, G., Lassey, K.R., Klusman, R.W., Boschi, E.: Reappraisal of the Fossil Methane Budget and Related
665 Emission from Geologic Sources, *Geophys. Res. Lett.*, 35, ISSN 1944-8007, 2008.
- 666 Haeckel, M., Boudreau, B. P., Wallmann, K.: Bubble-induced porewater mixing: A 3-D model for deep porewater
667 irrigation, *Geochim Cosmochim. Acta*, 71, 5135-5154, 2007.
- 668 Harvey, E. T., Kratzer, S., Philipson, P.: Satellite-based water quality monitoring for improved spatial and temporal retrieval
669 of chlorophyll-a in coastal waters, *Remote Sens. Environ.*, 158, 417-430, 2015.
- 670 Iversen, N., Jørgensen, B. B.: Diffusion coefficients of sulfate and methane in marine sediments: Influence of porosity,
671 *Geochim. Cosmochim. Acta* 57, 571-578, 1994.
- 672 Jørgensen, B. B. and Kasten, S.: Sulfur Cycling and Methane Oxidation, In: *Marine Geochemistry*, (Eds.) Schulz H. and
673 Zabel, M., Springer, Berlin Heidelberg, 271-309, 2006.

- 674 Jørgensen, B. B.: A comparison of methods for the quantification of bacterial sulfate reduction in coastal marine sediments,
675 *Geomicrobiol. J.*, 1, 11-27, 1978.
- 676 Jørgensen, B. B. and Parkes, R. J.: Role of sulfate reduction and methane production by organic carbon degradation in
677 eutrophic fjord sediments (Limfjorden, Denmark), *Limnol. Oceanogr.*, 55, 1338-1352, 2010.
- 678 Jonsson, P., Persson, J., Holmberg, P.: Skärgårdens bottenar, Report of the Swedish Environmental Protection Agency,
679 Stockholm, No. 5212, 114, 2003.
- 680 Judd, A. G.: Natural seabed gas seeps as sources of atmospheric methane, *Environ. Geol.*, 46, 988-996, 2004.
- 681 Kallmeyer, J., Ferdeman, T. G., Weber, A., Fossing, H., Jørgensen, B. B.: Evaluation of a cold chromium distillation
682 procedure for recovering very small amounts of radiolabeled sulfide related to sulfate reduction measurements,
683 *Limnol. Oceanogr. Meth.*, 2, 171-180, 2004.
- 684 Kampbell, D. H., Wilson, J. T., Vandegrift, S. A.: Dissolved Oxygen and Methane in Water by a GC Headspace
685 Equilibration Technique, *Intern. J. Environ. An. Ch.*, 36, 249-257, 1989.
- 686 Karlsson, M., M. Malmaeus, M., Rydin, E., Jonsson, P.: Bottenundersökningar i Upplands, Stockholms, Södermanlands
687 och Östergötlands skärgårdar: 2008-2009. Svenska Miljöinstitut, B1928, 102, 2010.
- 688 King, G.M.: Ecological Aspects of Methane Oxidation, a Key Determinant of Global Methane Dynamics, In: *Advances in*
689 *Microbial Ecology*, 12, Marshall, K.C. (ed.), 431-468, 1992.
- 690 Kirschke, S., Bousquet, P., Ciais, P., Saunois, M., Canadell, J.G., Dlugokencky, E.J., Bergamaschi, P., Bergmann, D.,
691 Blake, D.R., Bruhwiler, L.: Three Decades of Global Methane Sources and Sinks, *Nat. Geosci.*, 6, 813-23, 2013.
- 692 Knab, N. J., Cragg, B. A., Borowski, C., Parkes, R. J., Pancost, R. and Jørgensen, B. B.: Anaerobic oxidation of methane
693 (AOM) in marine sediments from the Skagerrak (Denmark): I. Geochemical and microbiological analyses.
694 *Geochim. Cosmochim. Acta*, 72, 2868-2879, 2009.
- 695 Knittel, K. and Boetius, A.: Anaerobic Oxidation of Methane: Progress with an Unknown Process. *Ann. Rev. Microbiol.*,
696 63: 311-334, 2009.
- 697 Klump, J. V. and Martens, C. S.: Biogeochemical cycling in an organic rich coastal marine basin—II. Nutrient sediment-
698 water exchange processes. *Geochim. Cosmochim. Acta*, 45, 101-121, 1981.
- 699 Kristensen, E., Bouillon, S., Dittmar, T., Marchand, C.: Organic carbon dynamics in mangrove ecosystems: A review.
700 *Aquat. Bot.*, 89, 201-219, 2008.
- 701 Larsson, U., Nyberg, U., Högländer, H., Sjösten, A., Sandberg, M., Walve, J.: Himmerfjärdens miljörapport 2012,
702 Department of Ecology, Environment, and Plant Sciences, Technical Report 50, 75, 2012.
- 703 Leloup, J., Fossing, H., Kohls, K., Holmkvist, L., Borowski, C., Jørgensen, B. B.: Sulfate-reducing bacteria in marine
704 sediment (Aarhus Bay, Denmark): abundance and diversity related to geochemical zonation. *Environ. Microbiol.*,
705 11, 1278-1291, 2009.
- 706 Martens, C. S., Albert, D. B., Alperin, M. J.: Biogeochemical processes controlling methane in gassy coastal sediments -
707 Part I. A model coupling organic matter flux to gas production, oxidation, and transport. *Cont. Shelf Res.*, 18,
708 1741-1770, 1998.
- 709 Martens, C. S. and Berner, R. A.: Methane production in the interstitial waters of sulfate-depleted marine sediments.
710 *Science*, 185, 1167-1169, 1974.
- 711 Martens, C. S. and Klump, J.: Biogeochemical cycling in an organic-rich coastal marine basin. 4. An organic carbon budget
712 for sediments dominated by sulfate reduction and methanogenesis. *Geochim. Cosmochim. Acta*, 48, 1987-2004,
713 1984.
- 714 Martens, C.S. and Val Klump, J.: Biogeochemical cycling in an organic-rich coastal marine basin—I. Methane sediment-
715 water exchange processes. *Geochim. Cosmochim. Acta*, 44, 471-490, 1980.
- 716 Marty, D., Bonin, P., Michotey, V. and Bianchi, M.: Bacterial biogas production in coastal systems affected by freshwater
717 inputs. *Cont. Shelf Res.*, 21, 2105-2115, 2001.
- 718 McDonald, I. R., Smith, K., Lidstrom, M. E.: Methanotrophic populations in estuarine sediment from Newport Bay,
719 California, *FEMS Microbiol. Lett.*, 250, 287-293, 2005.
- 720 Middelburg, J., Nieuwenhuize, J., Iversen, N., Høgh, N., de Wilde, H., Helder, W., Seifert, R. and Christof, O.: Methane
721 distribution in European tidal estuaries, *Biogeochemistry*, 59, 95-119, 2002.
- 722 Mogollón, J. M., Dale, A. W., L'Heureux, I., Regnier, P.: Impact of seasonal temperature and pressure changes on methane
723 gas production, dissolution, and transport in unfractured sediments, *J. Geophys. Res. Biogeosci.*, 116, G03031,
724 2011.
- 725 Moussard, H., Stralis-Pavese, N., Bodrossy, L., Neufeld, J. D., Murrell, J. C.: Identification of active methylotrophic
726 bacteria inhabiting surface sediment of a marine estuary, *Environ. Microbiol. Repts.*, 1, 424-433, 2009.
- 727 Musenze, R.S., Werner, U., Grinham, A., Udy, J. and Yuan, Z.: Methane and nitrous oxide emissions from a subtropical
728 estuary (the Brisbane River estuary, Australia), *Sci. Total Environ.*, 472, 719-729, 2014.

- 729 Nguyen, T.D., Crill, P. and Bastviken, D.: Implications of temperature and sediment characteristics on methane formation
730 and oxidation in lake sediments, *Biogeochemistry* 100, 185-196, 2010.
- 731 Norkko, J., Gammal, J., Hewitt, J., Josefson, A., Carstensen, J., Norkko, A.: Seafloor Ecosystem Function Relationships: In
732 Situ Patterns of Change Across Gradients of Increasing Hypoxic Stress, *Ecosystems* 18, 1424-1439, 2015.
- 733 Persson, J., Jonsson, P.: Historical development of laminated sediments—an approach to detect soft sediment ecosystem
734 changes in the Baltic Sea. *Mar. Poll. Bull.*, 40, 122-134, 2000.
- 735 Reeburgh, W. S.: Oceanic Methane Biogeochemistry, *Chem. Rev.*, 107, 486-513, 2007.
- 736 Reindl, A. R. and Bolalek, J.: Methane flux from sediment into near-bottom water and its variability along the Hel
737 Peninsula—Southern Baltic, Sea, *Cont. Shelf Res.*, 74, 88-93, 2014.
- 738 Savage, C., Leavitt, P. R., Elmgren, R.: Effects of land use, urbanization, and climate variability on coastal eutrophication in
739 the Baltic Sea. *Limnol. Oceanogr.*, 55, 1033-1046, 2010.
- 740 Sansone, F. J., Holmes, M. E. and Popp, B. N.: Methane stable isotopic ratios and concentrations as indicators of methane
741 dynamics in estuaries. *Global Biogeochem. Cycles*, 13, 463-474, 1999.
- 742 Sansone, F. J., Rust, T. M. and Smith, S. V., 1998. Methane Distribution and Cycling in Tomales Bay, California, *Estuaries*,
743 21, 66-77.
- 744 Seeberg-Elverfeldt, J., Schlüter, M., Feseker, T., Kölling, M.: Rhizon sampling of porewaters near the sediment-water
745 interface of aquatic systems. *Limnol. Oceanogr. Meth.*, 3, 361-371, 2005.
- 746 Smith, R.W., Bianchi, T.S., Allison, M., Savage, C., Galy, V.: High rates of organic carbon burial in fjord sediments
747 globally. *Nature Geosci.*, 8, 450-453, 2015.
- 748 Söderberg, P. and Flodén, T.: Gas seepages, gas eruptions and degassing structures in the seafloor along the Strömme
749 tectonic lineament in the crystalline Stockholm Archipelago, east Sweden. *Cont. Shelf Res.* 12, 1157-1171, 1992.
- 750 Stridh, S.: SYVAB Himmerfjärdsverket Miljörapport 2012, www.syvab.se/information/dokument/syvabs-miljorapporter,
751 53, 2012.
- 752 Thang, N., Brüchert, V., Formolo, M., Wegener, G., Ginters, L., Jørgensen, B. B., and Ferdelman, T.: The Impact of
753 Sediment and Carbon Fluxes on the Biogeochemistry of Methane and Sulfur in Littoral Baltic Sea Sediments
754 (Himmerfjärden, Sweden), *Estuaries and Coasts*, 36, 98-115, 2013.
- 755 Tóth, Z., Spiess, V., Keil, H.: Frequency dependence in seismoacoustic imaging of shallow free gas due to gas bubble
756 resonance, *J. Geophys. Res. Solid Earth*, 120, 8056-8072, 2015.
- 757 Treude, T., Krüger, M., Boetius, A., Jørgensen, B. B.: Environmental control on anaerobic oxidation of methane in the
758 gassy sediments of Eckernförde Bay (German Baltic), *Limnol. Oceanogr.*, 50, 1771-1786, 2005a.
- 759 Treude, T., Niggemann, J., Kallmeyer, J., Wintersteller, P., Schubert, C. J., Boetius, A., and Jørgensen, B. B.: Anaerobic
760 oxidation of methane and sulfate reduction along the Chilean continental margin, *Geochim. Cosmochim. Acta*, 69,
761 2767-2779, 2005b.
- 762 Upstill-Goddard, R. C., Barnes, J., Frost, T., Punshon, S. and Owens, N. J. P.: Methane in the southern North Sea: Low-
763 salinity inputs, estuarine removal, and atmospheric flux, *Global Biogeochem. Cycles*, 14, 1205-1217, 2000.
- 764 Valentine, D.L.: Emerging Topics in Marine Methane Biogeochemistry. *Annual Rev. Mar. Sci.*, 3, 147-171, 2011.
- 765 Wegener, G., Bausch, M., Holler, T., Thang, N. M., Prieto Mollar, X., Kellermann, M. Y., Hinrichs, K. U., and Boetius, A.:
766 Assessing sub-seafloor microbial activity by combined stable isotope probing with deuterated water and ¹³C-
767 bicarbonate. *Environ. Microbiol.*, 14, 1517-1527, 2012.
- 768 Westrich, J. T., Berner, R. A.: The role of sedimentary organic matter in bacterial sulfate reduction: The G model tested.
769 *Limnol. Oceanogr.*, 29, 236-249, 1984.
- 770 Wik, M., Thornton, B.F., Bastviken, D., MacIntyre, S., Varner, R.K. and Crill, P.M.: Energy input is primary controller of
771 methane bubbling in subarctic lakes. *Geophysical Research Letters* 41, 555-560, 2014.
- 772 Wilhelm, E., Battino, R., and Wilcock, R. J.: Low-pressure solubility of gases in liquid water. *Chem. Rev.*, 77, 219-262,
773 1977.
- 774 Zakrisson, A., and Larsson, U.: Regulation of heterocyst frequency in Baltic Sea *Aphanizomenon* sp., *J. Plankton Res.*, 36,
775 1357-1367, 2014.
- 776 Zhang, G., Zhang, J., Liu, S., Ren, J., Xu, J. and Zhang, F.: Methane in the Changjiang (Yangtze River) estuary and its
777 adjacent marine area: riverine input, sediment release and atmospheric fluxes. *Biogeochemistry*, 91, 71-84, 2008.
- 778 Zhang, W., Bougouffa, S., Wang, Y., Lee, O. O., Yang, J., Chan C. Song, X., and Qian, P.-Y.: Toward understanding the
779 dynamics of microbial communities in an estuarine system, *PLoS ONE*, 9, e94449, 2014.
- 780

781 **Table 1.** Main site characteristics of the sampling stations.

Station	Sampling time	Water depth (m)	Temperature (°C)	Bottom water salinity (‰)	Bottom water Oxygen (µM)	Surface organic carbon (%)
B1 58°48'18"N 17°37'52"E	April 2012	41	2.4	6.5	160	6.0
	August 2012		6.9	7.0	260	5.2
	October 2012		6.8	7.0	224	5.1
	February 2013		3.4	7.0	380	5.0
H6 59°04'08"N 17°40'63"E	April 2012	39.5	1.8	5.9	40	4.6
	August 2012		6.7	6.4	150	5.1
	October 2012		9.4	6.5	191	5.2
	February 2013		1.8	5.4	300	4.7

782

783

784

785

786

787

788

789

790

Table 2. Summary of CH₄ and SO₄²⁻ fluxes, depth-integrated ³⁵SRR, and total oxygen uptake (TOU).

Station	Sampling time	Flux (mmol m ⁻² d ⁻¹)						Integrated ³⁵ S-SRR (n=3)
		TOU whole core incubation (n=4)	CH ₄ whole core incubation (n=4)	CH ₄ Diffusive flux to sediment surface (n=1)	CH ₄ Diffusive flux into SMTZ (n=1) ²	SO ₄ ²⁻ Diffusive flux into sediment (n=1)	³⁵ S-SRR integrated over AOM ³ zone (n=3)	
B1	April 2012	19.7±2.5	-0.10±0.05	-0.1		0.4	no AOM zone ⁴	2.3±0.6
	August 2012	22.5±2.9	-1.2±0.6	-(0.01)		0.8	no AOM zone ⁴	0.5±0.1
	October 2012	21.1±2.7	No data	-0.3		1.4	no AOM zone ⁴	2.0±0.0.5
	February 2013	12.0±1.5	-0.1±0.05	-0.02		0.2	no AOM zone ⁴	2.2±0.6
H6	April 2012	33.5±3.5	-0.3±0.1	-1.7	-2.8	2.6	(10-18 cm) =	11.6±2.9
	April 2013		-3.9 ±0.7 ¹				-2.8±0.7	
	August 2012	26.9±2.8	-19.9±7.8 ⁵	-2.3	-2.6	2.7	(10-18 cm) =	11.7±2.9
	October 2012	25.9±2.7	-1.0	-2.0	-1.9	2.6	(10-18 cm) =	11.5±2.9
	February 2013	14.9±1.6	-1.1	-0.5	-0.4	1.3	no AOM zone ³	9.2±2.3

791

¹ whole core incubation was performed in April 2013; Diffusive fluxes were calculated for samples collected in April 2012;

792

² SMTZ - sulfate methane transition zone, ³ AOM zone – zone of anaerobic oxidation of methane, ⁴ no AOM zone means

793

that AOM zone was probably deeper than the core length; ⁵ potentially elevated due to depressurization/ex-solution

794

effect during core incubation at atmospheric pressure;

795

796 **Table 3.** Best-fit regression coefficients a and b for the depth gradient of sulfate
 797 reduction rates ($^{35}\text{SRR} = az^b$ (z =depth, cm)).

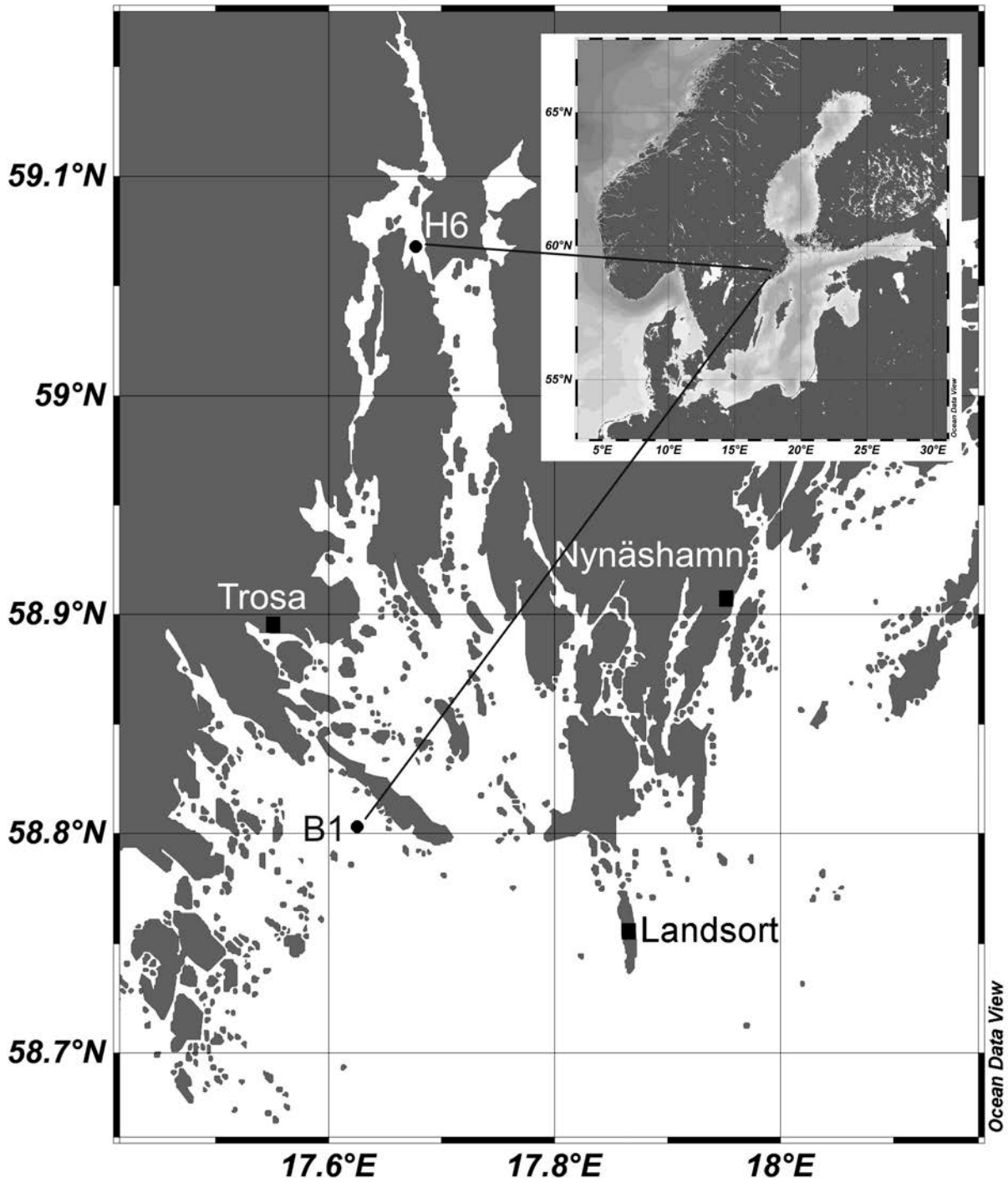
Station	Sampling time	Exponential coefficient (a)	Exponential coefficient (b)
B1	April 2012	147.0	-1.4
	August 2012	11.7	-0.9
	October 2012	16.0	-0.4
	February 2013	33.5	-0.8
H6	April 2012	18.6	-0.5
	August 2012	37.4	-0.5
	October 2012	133.2	-0.8
	February 2013	25.0	-0.4

798

799

800

801



802

Figure 1. Location of sampling sites in Himmerfjärden, Stockholm Archipelago, Sweden. Detailed studies were conducted at two sites, an open water site (station B1) and in the inner part of the estuary (station H6).

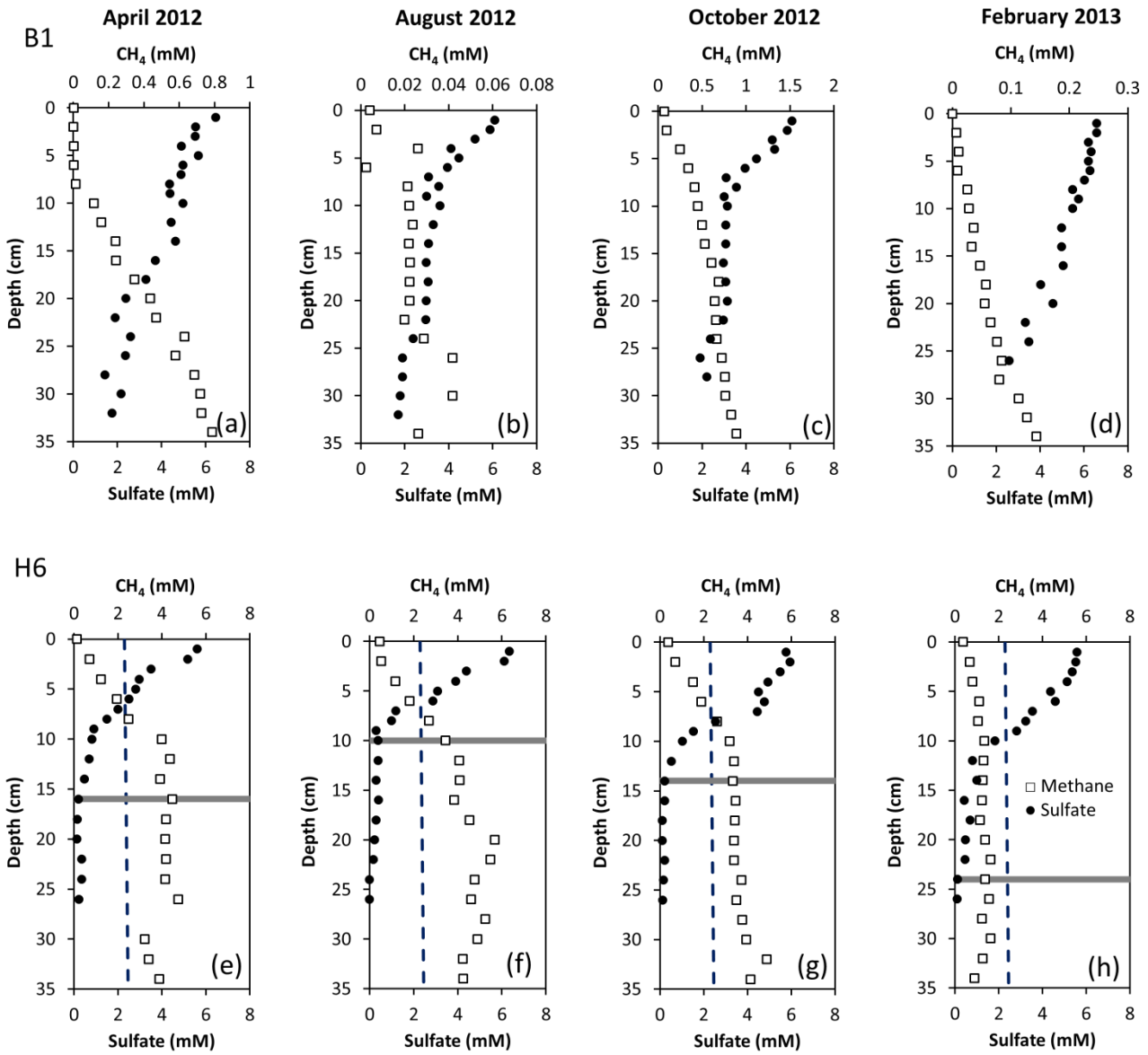


Figure 2. Porewater profiles of total methane and sulfate at Station B1 (a-d) and Station H6 (e-h) for the different sampling periods. The grey line marks the initial minimum sulfate concentration depth. Dashed lines indicate the methane saturation concentration at 1 atm pressure (grey) at the time of sampling. All concentrations of methane are below the in situ saturation concentration of methane (see text for details).

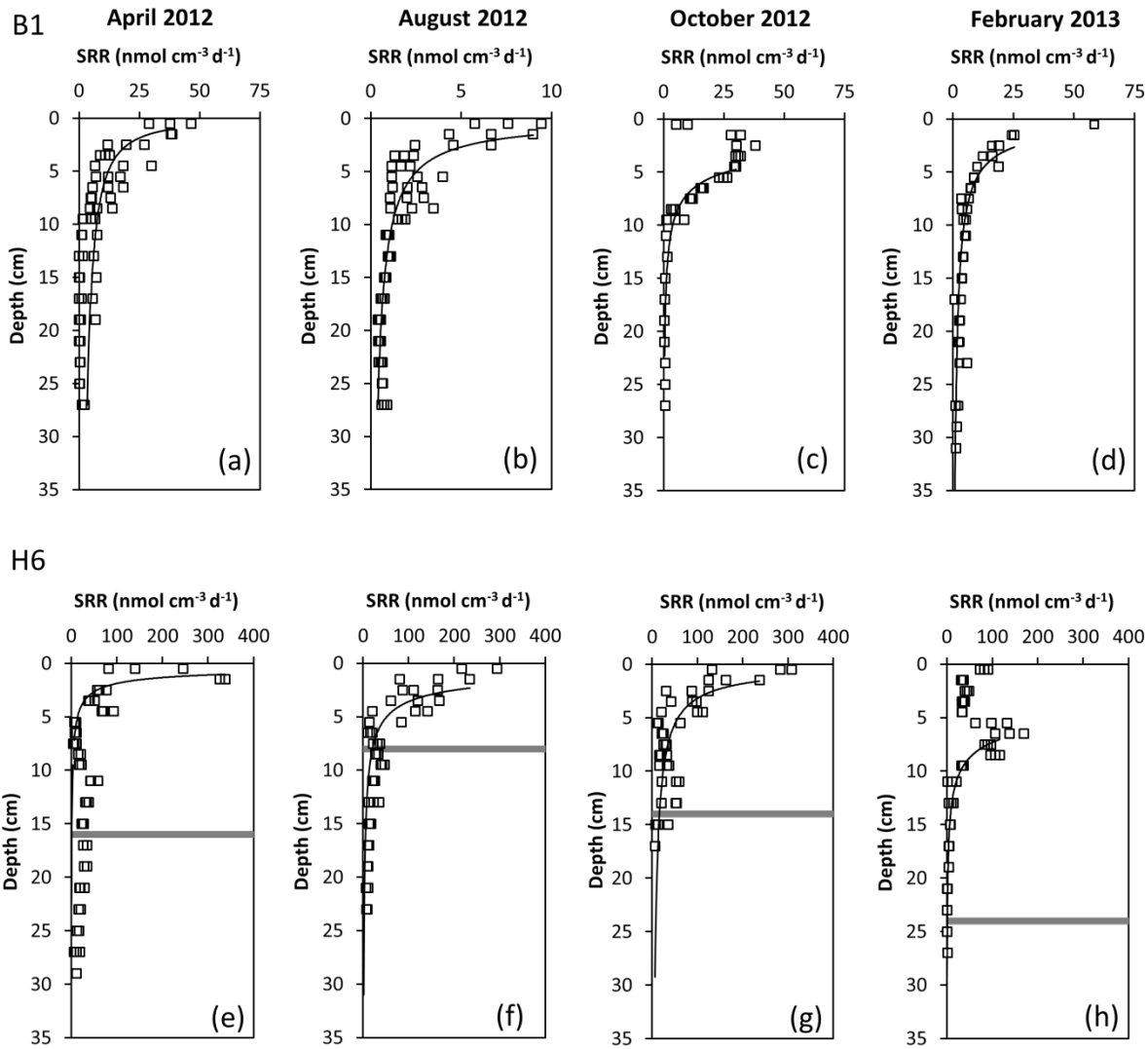


Figure 3. Depth gradients of bacterial sulfate reduction rates (SRR) measured with ^{35}S -sulfate at Station B1 (a-d) and Station H6 (e-h) for the different sampling periods. Black lines show the regression results to a power function of the form $y = ax^{-b}$. The grey line marks the initial minimum sulfate concentration depth.

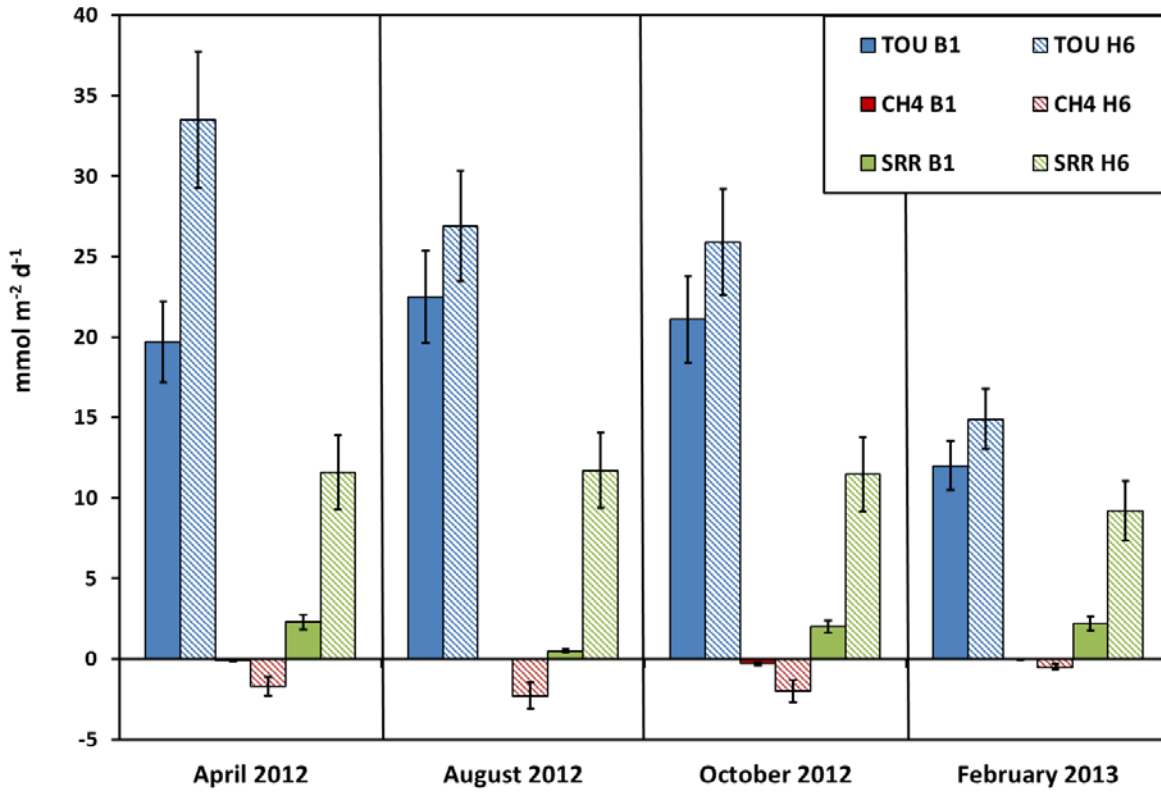


Figure 4. Comparison of benthic fluxes ($\text{mmol m}^{-2} \text{d}^{-1}$) for sulfate (SO_4), methane (CH_4), and oxygen (TOU) for the different sampling periods.

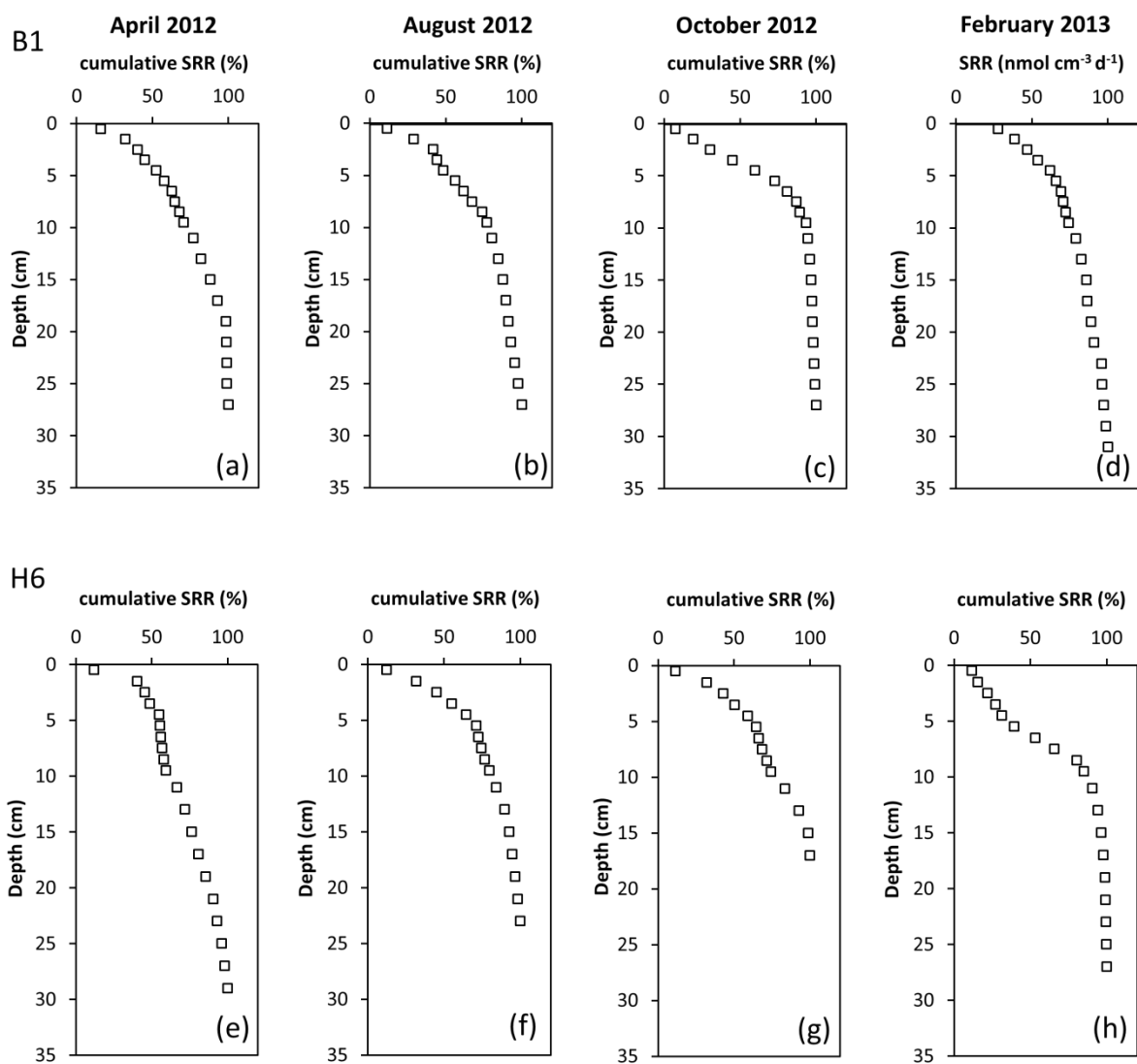


Figure 5. Depth distribution of sulfate reduction rate expressed as cumulative percentage at Station B1 (a-d) and Station H6 (e-h) for the different sampling periods. The grey line marks the initial minimum sulfate concentration depth.